ISSN 1063-7834, Physics of the Solid State, 2017, Vol. 59, No. 8, pp. 1558–1564. © Pleiades Publishing, Ltd., 2017.
Original Russian Text © V.S. Pokatilov, V.S. Rusakov, A.S. Sigov, A.A. Belik, 2017, published in Fizika Tverdogo Tela, 2017, Vol. 59, No. 8, pp. 1535–1541.

Mössbauer Studies of Multiferroics $BiFe_{1-x}Cr_xO_3$ ($x = 0–0.20$)

V. S. Pokatilov[a,*], **V. S. Rusakov**[b], **A. S. Sigov**[a], **and A. A. Belik**[c]
[a] *Moscow Technological University (MIREA), pr. Vernadskogo 78, Moscow, 119454 Russia*
[b] *Moscow State University, Moscow, 119991 Russia*
[c] *International Center for Materials Nanoarchitectonics (WRI–MANA),*
National Institute for Materials Science (NIMS), Tsukuba, Ibaraku, Japan
**e-mail: pokatilov@mirea.ru*

Received December 8, 2016; in final form, February 9, 2017

Abstract—The Mössbauer studies on ^{57}Fe nuclei in multiferroics $BiFe_{1-x}Cr_xO_3$ ($x = 0.05$, 0.10, and 0.20) have been performed at room temperature. The multiferroics $BiFe_{1-x}Cr_xO_3$ ($x = 0.05$, 0.10, and 0.20) with the rhombohedral $R3c$ structure have been prepared by solid-state synthesis under high pressures. The effect of substitution of Cr cations for Fe cations on the spatial spin-modulated structure, and also hyperfine electrical and magnetic interactions of ^{57}Fe nuclei has been studied. The substituted ferrites demonstrate an anharmonic modulated spin structure of cycloid type, in which iron atoms with different cation environments take part. The anharmonism parameter of the cycloid linearly increases from $m = 0.10$ at $x = 0$ to $m = 0.78 \pm 0.02$ at $x = 0.20$. The constants of magnetic uniaxial anisotropy K_u are estimated at room temperature: $K_u \approx 0.36 \times 10^6$ erg/cm^3 at $x = 0$ and $K_u \approx 4.22 \times 10^6$ erg/cm^3 at $x = 0.20$.

DOI: 10.1134/S1063783417080194

1. INTRODUCTION

At present, materials called multiferroics attract a great interest from researchers. This interest is due to the nature of fundamental physical properties and also a great potential of these materials for applications in practice [1–4]. Multiferroics $BiFeO_3$ is of the highest interest, since it has the magnetic and electric transition temperatures higher than room temperature [1–4].

However, $BiFeO_3$ has no a weak ferromagnetism and, as a result, linear magnetoelectric effect [6] because of the spatial spin-modulated structure (SSMS) of the cycloid type with the wavelength 620 Å [5]. The disturbance or suppression of the SSMS cycloid, e.g., by external magnetic field of 200 kOe, led to the increase in the magnetization and the appearance of a linear magnetoelectric effect [7]. The magnetoelectric properties of multiferroics $BiFeO_3$ were also improved by substitution of cations of various groups of the periodic table of elements for Bi or Fe cations (for example, [8–10]).

Double perovskites of the $A_2BB'O_6$ type, in particular, the $BiFeO_3$–$BiCrO_3$ system generate a great interest. According to [11], as chromium cations substitute iron cations in double perovskites, the Fe^{3+}–O–Cr^{3+} spin bond can create ferromagnetic ordering. The magnetic structure and the ferroelectric polarization in the ordered Bi_2FeCrO_6 were calculated in [12]. It was predicted that the magnetic and electrical properties of the double perovskite can be improved by the ordering of cations Fe^{3+} and Cr^{3+}. The experimental studies of the bulk perovskite Bi_2FeCrO_6 did not reveal any improvement of its magnetic and electrical properties, since it turned out that cations Fe^{3+} and Cr^{3+} in the bulk perovskite Bi_2FeCrO_6 samples were randomly distributed over positions B and B' [13]. High values of the electric polarization and the magnetization were observed in thin films, nanostructures, and superlattices of perovskites Bi_2FeCrO_6 and $BiFe_{1-x}Cr_xO_3$ at room temperature [14–18]. However, these effects were obtained as a result of the influence of various defects, stresses, lattice distortions, impurities, other crystalline impurity phases and other factors, not due to an ordering of cations Fe^{3+} and Cr^{3+}. The increase in the magnetization in thin films, nanostructures, and superlattices was explained by the ferro- and antiferromagnetic bonds in Fe–O–Fe/Cr chains, since these bonds were significantly dependent on the magnitude and the angle of the superexchange interactions between cations Fe^{3+} and Fe^{3+}/Cr^{3+} (e.g., [14–18].

The study of the magnetic states of iron cations and SSMS in bulk perovskites $BiFe_{1-x}Cr_xO_3$ ($x = 0.05$, 0.10, and 0.20) is of certain interest, since bulk samples of this system can be free from various defects, stresses, and other factors, which are the cause of changing the physical properties observed in the films, nanostructures, and superlattices. It is difficult to prepare single-phase bulk samples in the $BiFe_{1-x}Cr_xO_3$

Table 1. Lattice parameters in the rhombohedral samples of multiferroics $BiFe_{1-x}Cr_xO_3$ ($x = 0.05$, 0.10, and 0.20)

x	a (Å)	c (Å)
0.00	5.5795(1)	13.8686(2)
0.05	5.5762(1)	13.8564(2)
0.10	5.5730(1)	13.8410(2)
0.20	5.5674(1)	13.8130(2)

system using common solid-phase synthesis technologies at normal pressure. Single-phase bulk samples of the $BiFe_{1-x}Cr_xO_3$ system were prepared by solid-phase synthesis under high pressures [13–15], the sol gel method, and the combustion method [16–18]. As follows from [13–15], the substitution of chromium cations for iron cations decreased the lattice parameters and increased the magnetization. In [13, 18], the Mössbauer effect was studied in the multiferroics $BiFe_{1-x}Cr_xO_3$ and it was found the iron cations in bulk samples and nanoparticles of $BiFe_{1-x}Cr_xO_3$ ($x = 0$, 0.05, and 0.10) were in a trivalent state. However, the influence of the substitution of chromium cations for iron cations on the SSMS parameters and the parameters of the hyperfine interactions on ^{57}Fe nuclei in multiferroics $BiFe_{1-x}Cr_xO_3$ was not studied.

This work presents the results of studies, at room temperature, of the crystal structure and the Mössbauer effect on ^{57}Fe nuclei of bulk $BiFe_{1-x}Cr_xO_3$ ($x =$ 0.05, 0.10, and 0.20) samples synthesized under high pressures.

2. EXPERIMENTAL

Multiferroics $BiFe_{1-x}Cr_xO_3$ ($x = 0.05$, 0.10, and 0.20) samples were prepared from the stoichiometric mixture of Bi_2O_3 (99.9999% pure), Fe_2O_3 (99.999%), $^{57}Fe_2O_3$ (95.5% ^{57}Fe) with the concentration of 10 mol %, and Cr_2O_3 (99.99% pure). At the initial stage, the mixture was annealed at a temperature of 1250 K and a pressure of 6 GPa for 1.5 h in hermetically sealed gold capsules. Then, the homogenizing annealing was performed at $T = 800$ K for 2 h. After the temperature annealing, the sample was slowly cooled to room temperature. The synthesis was performed in the International Center for Materials Nanoarchitectonics at the National Institute for Materials Science (Japan). The X-ray diffraction data were obtained at room temperature using a RIGAKU Ultima III diffractometer. The photography was performed in the range of diffraction angles 0–65° with a pitch and a measurement time of 2–10 s/step.

The Mössbauer studies were performed using an MS1104Em spectrometer operating in the constant acceleration mode with a triangular form of the change in the Doppler velocity of the source with respect to the absorber. The sources were ^{57}Co nuclei in the *Rh* matrix. The Mössbauer spectrometer was calibrated at room temperature using an α-Fe standard absorber. The spectra of the samples were measured at room temperature. The Mössbauer spectra were processed and analyzed using the method of interpretation of spectra in terms of the SSMS model of cycloid type described in [19, 20] and used in the SpectrRelax program [21, 22].

3. EXPERIMENTAL RESULTS AND DISCUSSION

Figure 1 depicts the X-ray diffraction spectrum of the $BiFe_{0.90}Cr_{0.10}O_3$ sample measured at room temperature (as an example). Table 1 gives the lattice parameters of multiferroics $BiFe_{1-x}Cr_xO_3$ ($x = 0.05$, 0.10, and 0.20) samples. The sample structure was rhombohedral. The lattice parameters decreased as the chromium content increased. These data agreed with the data of [13–18]. The substitution of chromium cations for iron cations in multiferroics $BiFe_{1-x}Cr_xO_3$ ($x = 0.05$, 0.10, and 0.20) decreased the lattice parameters. This effect was due to that the effective cation radius of trivalent chromium cation ($R(Cr^{+3}) = 0.615$ Å) was significantly smaller than the effective cation radius of trivalent iron cation ($R(Fe^{+3}) = 0.645$ Å) [23]. The samples studied contained small amounts of impurity phases $Bi_2O_2CO_3$ and Fe_2O_3.

Figure 2 shows the Mössbauer spectra of the multiferroics $BiFe_{1-x}Cr_xO_3$ ($x = 0.05$, 0.10, and 0.20). The spectra of the samples exhibiting SSMS of the cycloid type measured at temperatures below than the Néel temperature demonstrated the features that were observed in the Mössbauer spectra of $BiFeO_3$ [19, 20] and $BiFe_{1-x}T_xO_3$ (T = Sc, Mn) [24], namely, an asymmetry of the Zeeman sextet with nonuniformly broadened resonance lines. These features were related to the existence in the spectrum of a positive correlation of the hyperfine magnetic field and the quadrupole shift of the resonance lines due to rotation of Fe atom spin in SSMS of cycloid type considered in detail in [19–22, 24]. The resonance lines in the spectra of the substituted perovskites $BiFe_{1-x}Cr_xO_3$ ($x =$ 0.05, 0.10, and 0.20) were more broadened as compared to the lines in the spectrum of pure $BiFeO_3$ [19, 20] and $BiFe_{1-x}T_xO_3$ (T = Sc, Mn) [24].

Dependence $\vartheta(x)$ of the angle between the antiferromagnetism vector and the symmetry axis in the structure of bismuth ferrite $BiFeO_3$ on coordinate x along the spin modulation direction for the positive sign of the coefficient of the uniaxial magnetic anisotropy K_u (in more detail, the sign of K_u was discussed in [25]) is described by equation

$$\cos\vartheta(x) = \mathrm{sn}\left(\frac{4K(m)}{\lambda}x, m\right) \quad \text{at} \quad K_u > 0, \qquad (1)$$

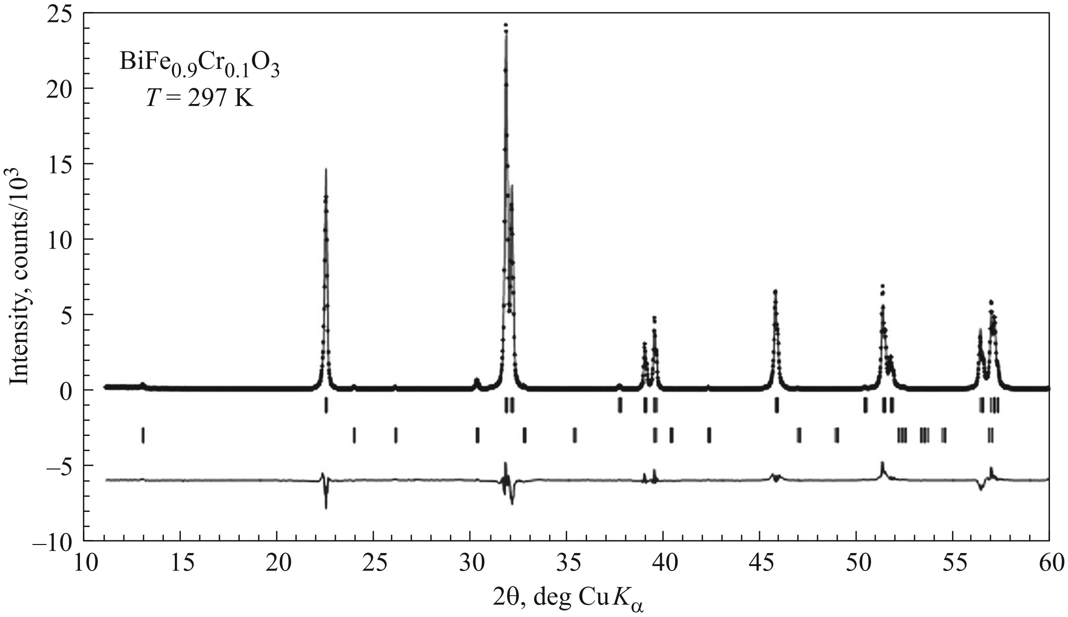

Fig. 1. X-ray diffraction pattern of the $BiFe_{0.95}Cr_{0.05}O_3$ sample.

where λ is the wavelength of the anharmonic spin modulation, $0 \le m \le 1$ is the Jacobian function parameter $sn(x, m)$ (m is the parameter of anharmonism of the incommensurable spin modulation), and $K(m)$ is the first order complete elliptic integral. The SSMS wavelength λ is related by Eq. (2) to the energy constants of the thermodynamic potential: with the coefficient of the uniaxial magnetic anisotropy K_u characterizing the energy of the uniaxial magnetic anisotropy $E_a = K_u\sin^2\vartheta$, exchange hardness A characterizing the energy of nonuniform exchange interaction $E_{exch} = Aq^2$, where A is the nonuniform exchange constant (excharge hardness) and $q = 2\pi/\lambda$ is the wave number

$$\lambda = 4(A/K_u)^{1/2}K(m)m^{1/2}. \quad (2)$$

The Mössbauer spectra of the $BiFe_{1-x}Cr_xO_3$ (x = 0.05, 0.10, and 0.20) system samples were processed in the framework of the SSMS model of cycloid type. The main positions of this model for interpretation of the Mössbauer spectra of $BiFeO_3$-based perovskites were presented in [19, 20, 24].

For every angle $\vartheta(x)$ from the range of varying coordinate $x \in [0, \lambda]$, there was resonant absorption line in the form of the Zeeman sextet with shift δ, quadrupole shifts of the first $\varepsilon(\vartheta)$ and the second $a_{\pm}(\vartheta)$ smallness orders in the expansion in terms of the energy of quadrupole interaction, and the hyperfine magnetic field (HFMF) $H_n(\vartheta)$. We considered quadrupole shift ε equal to the quadrupole shift induced by the electric field gradient generated by atoms surrounding the nucleus ε_{lat} and did not take into account additional possible shift ε_{magn} that was provided by a local distortion of the lattice because of a strong magnetoelectric interaction [21], since, as was shown in [19, 20], this additional shift can be neglected in the case of bismuth ferrite.

In the case of the uniaxial anisotropy of the hyperfine interaction when it is fairly small, as is the case with ^{57}Fe nuclei in $BiFeO_3$, the hyperfine magnetic field on ^{57}Fe nuclei $H_n(\vartheta)$ can be represented as

$$H_n(\vartheta) = H_{is} + H_{an}(3\cos^2(\vartheta) - 1)/2, \quad (3)$$

where H_{is} is the isotropic contribution to the hyperfine magnetic field H_n that is mainly determined by the contact Fermi interaction with s electrons localized at a nucleus and polarized by the atom spin, H_{an} is the anisotropic contribution provided by the magnetic dipole–dipole interaction with localized magnetic moments of atoms and the anisotropy of the hyperfine magnetic interaction of the nucleus and the electrons of the ion core of the proper atom. From Eq. (3), it follows that the values of the hyperfine magnetic fields in the case of the orientation of the iron atom magnetic moment in parallel ($H_{\parallel}$) and perpendicularly ($H_{\perp}$) to the crystal symmetry axis, which were used in [19, 20, 26], are related to the isotropic and anisotropic contributions by simple relationships $H_{\parallel} = H_{is} + H_{an}$ and $H_{\perp} = H_{is} - H_{an}/2$. The searching for optimal values of all the parameters of the hyperfine interaction (δ, ε_{lat}, H_{is}, and H_{an}) and the anharmonism parameter of spin modulation (m) was performed during the interpretation of the Mössbauer spectra in the framework of the SSMS model of cycloid type.

According to the interpretation, one partial spectrum in the SSMS model of cycloid type corresponded to the Mössbauer spectrum [19, 20]. To adequately

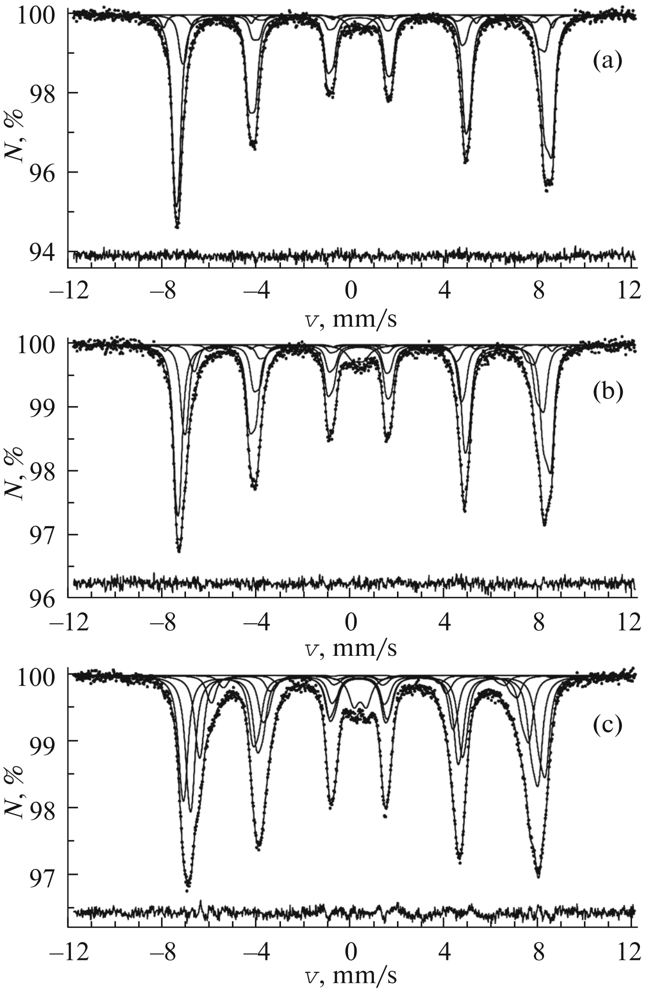

Fig. 2. Mössbauer spectra of ^{57}Fe nuclei of ferrites (a) $BiFe_{0.95}Cr_{0.05}O_3$, (b) $BiFe_{0.90}Cr_{0.10}O_3$ and (c) $BiFe_{0.80}Cr_{0.20}O_3$ measured at room temperature and the results of processing of the spectra in terms of the model of anharmonic spin wave.

describe the Mössbauer spectra in the substituted ferrites $BiFe_{1-x}Cr_xO_3$ (x = 0.05, 0.10, and 0.20) and according to the distribution of chromium cations over the iron cation positions, the nearest environment of which contained different numbers N_{Cr} of impurity chromium cations, we considered the existence of several most probable partial magnetic spectra. These partial spectra corresponded to the model of unique anharmonic spin wave in which spins of all iron atoms in the perovskites took part. In this case, line shifts δ, quadrupole shifts ε_{lat}, anisotropic contributions H_{an}, and the anharmonism parameters m of these partial spectra were taken to be the same, but isotropic contributions H_{is} were varied. The equalities of the widths (Γ) and intensities (I) of resonant lines in sextet were held in pairs: $\Gamma_1 = \Gamma_6$, $\Gamma_2 = \Gamma_5$, $\Gamma_3 = \Gamma_4$ and $I_1 = I_6$, $I_2 = I_5$, $I_3 = I_4$.

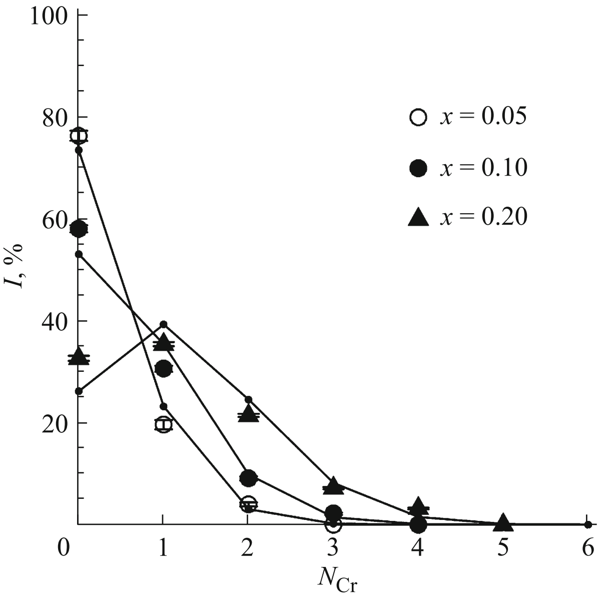

Fig. 3. Dependences of the relative intensities of the partial spectra of ^{57}Fe nuclei in ferrites $BiFe_{1-x}Cr_xO_3$ (x = 0.05, 0.10, and 0.20) on the number N_{Cr} of Cr atoms in the nearest cation environment of a Fe atom; points connected by lines are the binominal distribution $P_6(N_{Cr})$.

To adequate describe the spectra in the $BiFe_{1-x}Cr_xO_3$ (x = 0.05, 0.10, and 0.20) system, it was sufficient to have three partial spectra for the spectrum of the $BiFe_{0.95}Cr_{0.05}O_3$ sample, four partial spectra for the spectrum of the $BiFe_{0.90}Cr_{0.10}O_3$ sample, and five partial spectra for the spectrum of the $BiFe_{0.80}Cr_{0.20}O_3$ sample (Fig. 2). The envelopes of the model spectra corresponded well to the experimental Mössbauer spectra (normalized functional square was χ^2 = 1.0–1.2) with inclusions of the contributions of two low-intense partial spectra of impurity phases. Figure 3 shows the dependences of the relative intensities of the partial spectra of Fe^{3+} nuclei in perovskites $BiFe_{1-x}Cr_xO_3$ (x = 0.05, 0.10, and 0.20) on the number N_{Cr} of cations Cr in the nearest cation environment of a cation Fe; the points connected by lines were due to binominal distribution $P_6(N_{Cr})$. These data showed that chromium cations in multiferroics $BiFe_{1-x}Cr_xO_3$ (x = 0.05, 0.10, and 0.20) were randomly distributed in the lattice over the iron atom positions.

The model interpretation showed that the Mössbauer line shift δ (0.39 ± 0.01 mm/s) was almost independent of the chromium cation concentration in $BiFe_{1-x}Cr_xO_3$ (x = 0, 0.05, 0.10, and 0.20) and corresponded to a high spin state of iron cations Fe^{3+} in the octahedral oxygen environment. Quadrupole shift ε_{lat} provided by the electric field gradient induced by cations surrounding the nucleus decreased slightly as the cation Cr concentration increased from ε_{lat} = 0.236 ±

0.002 mm/s at $x = 0.05$ to $\varepsilon_{lat} = 0.219 \pm 0.009$ mm/s at $x = 0.20$. Since the mean interatomic distances decreased as the Cr atom concentration increased, the contributions of localized charges and dipole moments of ions must increase. It is likely that the decrease in the quadrupole shift was related to a decrease in the electron contribution [27] due to a change in the number of electrons participating in the transfer and the degree of overlapping of orbitals of the iron and oxygen atoms.

The substitution of trivalent chromium cations for trivalent iron cations in the Fe–O–Fe/Cr bond chains substantially changed SSMS at ^{57}Fe nuclei of the iron cations. Figure 4 shows the dependence of the isotropic contribution H_{is} in SSMS on the number N_{Cr} of chromium cations in the nearest environment of a Fe cation in the $BiFe_{1-x}Cr_xO_3$ ($x = 0.05$, 0.10, and 0.20) system. It is seen that these dependence for the first three values of N_{Cr} (0, 1, 2) were described well in a linear approximation. In other words, the model of additive contributions in H_{is} on ^{57}Fe nuclei from atoms of the nearest environment was valid at small substitution of Cr atoms for Fe atoms. In this case, the replacement of a Fe atom for a Cr atom changed field H_{is} by $\Delta H_{is} \cong -21.6$ kOe. The further replacement of Fe cations for 3 and 4 Cr cations in the Fe–O–Fe/Cr bond chains decreased isotropic contribution H_{is} by ~30–40 kOe (Fig. 4). The anisotropic contributions H_{an} in HFMF of the multiferroics $BiFe_{1-x}Cr_xO_3$ ($x = 0.05$, 0.10, and 0.20) were close to each other and were $H_{an} = 4.5 \pm 0.2$ kOe.

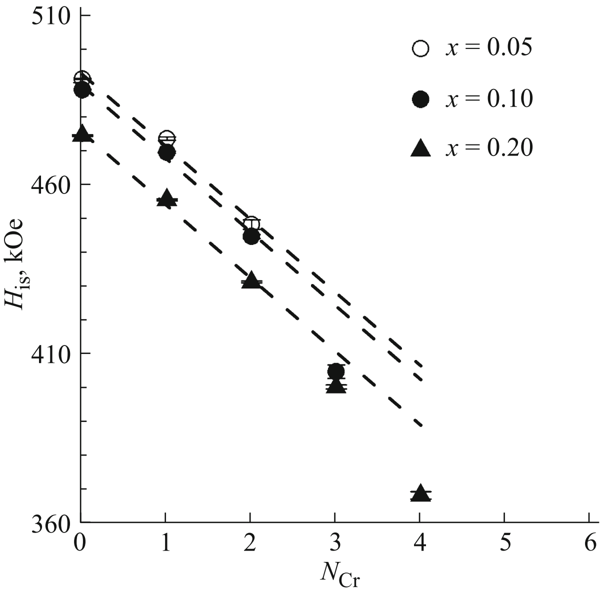

Fig. 4. Dependences of the isotropic contribution H_{is} to the hyperfine field on ^{57}Fe nuclei in multiferroics $BiFe_{1-x}Cr_xO_3$ ($x = 0.05$, 0.10, and 0.20) on the number N_{Cr} of Cr atoms in the nearest cation environment of a Fe atom.

According to [28–30], HFMF (H_{is}) on Fe^{3+} cation had two contributions. The main contribution H_{core} was due to the polarization of internal *s* electrons by a local magnetic moment $\mu(Fe^{3+})$ of the Fe^{3+} cation. This contribution was parallel to the local magnetic moment of the Fe^{3+} cation [28] and had the negative sign with respect to the direction of moment $\mu(Fe^{3+})$. Another contribution H_{cov} was due to covalence effect and consisted of two contributions [29, 30]. The first contribution in H_{cov} was H_{STHF} (supertransferred hyperfine field), i.e., HFMF on the central Fe^{3+} cation due to indirect influence of neighboring Fe^{3+} and Cr^{3+} cations on the central Fe^{3+} cation. In this case, H_{STHF} was determined by the covalence parameters of the Fe^{3+}–O^{2-} chemical bond and also by the angle in Fe–O–Fe and Fe–O–Cr chains. Another contribution H_c was dependent on the overlapping 2*p* orbitals O^{2-} with *ns* orbitals of Fe^{3+} and the transfer of electron spins from a metallic cation Fe^{3+} via oxygen to another metallic cation Fe^{3+} or Cr^{3+}. The decrease in the isotropic contribution H_{is} (Fig. 4) can be due to that the substitution of Cr^{3+} cations with smaller ionic radius for Fe^{3+} cations in the octahedral positions led to a distortion of oxygen octahedral to changes in the Fe–O–Fe and Fe–O–Cr bonds lengths and angles and to a change in the covalence parameters. The difference in the observed values of hyperfine magnetic fields for the states of the iron ions containing chromium ions in the nearest cation coordination sphere (Fig. 4) was related to various positive partial contributions H_{STHF} and H_c to HFMF on a ^{57}Fe nucleus in $BiFe_{1-x}Cr_xO_3$. It was difficult to estimate the influence of substitution of Cr^{3+} for Fe^{3+} on the local magnetic moment of cation Fe^{3+} $\mu(Fe^{3+})$ in the perovskite system under study, since there are no available data on magnetic moments of cations in the Fe^{3+}/Cr^{3+} positions. Magnetic moments $\mu(Fe^{3+})$ in $BiFeO_3$ were measured by neutron diffraction in [31] ($\mu(Fe) = 3.5\mu_B$ at room temperature and $\mu(Fe) = 4\mu_B$ at a temperature of 4.2 K). Magnetic moments of chromium cations $\mu(Cr)$ in $BiCrO_3$ were measured by neutron diffraction in [32, 33] ($\mu(Cr) = 2.55\mu_B$ at 7 K and $\mu(Cr) = 2.09\mu_B$ at 80 K [32]; $\mu(Cr) = 2.6\mu_B$ at a liquid helium temperature and $\mu(Cr) = 2.04\mu_B$ at 90 K [33]. It is likely that local magnetic moments $\mu(Cr)$ in the multiferroics $BiFe_{1-x}Cr_xO_3$ ($x = 0$, 0.05, 0.10, and 0.20) at room temperature have a smaller values than the iron moments of $\mu(Fe) = 3.5\mu_B$.

Figure 5 shows the dependence of the anharmonism parameter *m* of SSMS of cycloid type in the multiferroics $BiFe_{1-x}Cr_xO_3$ ($x = 0$, 0.05, 0.10, and 0.20) on the Cr cation concentration at room temperature. Parameter *m* was measured in $BiFeO_3$ at room temperature using the Mössbauer effect method in [19, 20] and it was $m = 0.10 \pm 0.03$. As chromium cation substi-

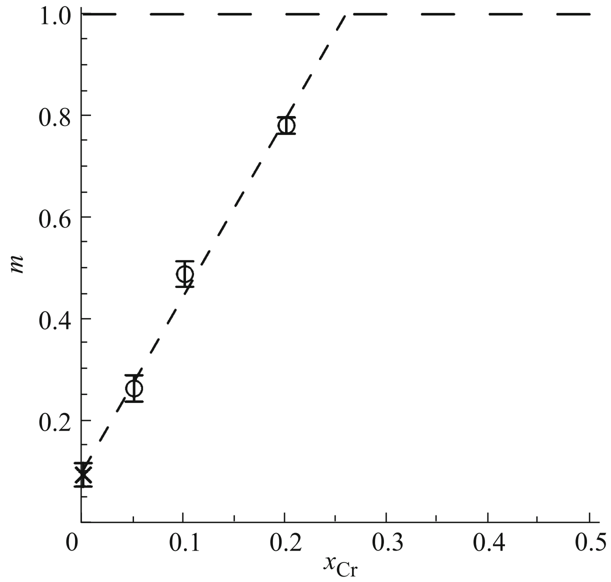

Fig. 5. Dependence of anharmonism parameter m of spin modulation in multiferroics $BiFe_{1-x}Cr_xO_3$ (x = 0.05, 0.10, and 0.20).

tuted iron cations in the perovskites $BiFe_{1-x}Cr_xO_3$ (x = 0.05, 0.10, and 0.20), parameter m linearly increased from $m = 0.26$ at $x = 0.05$ to $m = 0.78 \pm 0.02$ at $x = 0.20$. This effect demonstrates the increase in the anharmonism in SSMS upon substituting of chromium cations for iron cations in $BiFe_{1-x}Cr_xO_3$. The extrapolation of the values of the anharmonism parameter to the value $m = 1$ showed that, in the $BiFe_{1-x}Cr_xO_3$ system, the SSMS of cycloid type is likely to be disturbed at chromium content $x = 0.26$; i.e., the SSMS cycloidal structure with the G-type magnetic order is transformed to the G-type collinear antiferromagnetic structure.

The change in the anharmonism parameter m as chromium cations substitute iron cations was provided by a change in the constant of uniaxial magnetic anisotropy K_u and the energy of the nonuniform exchange interaction E_{exch}. We estimated the exchange hardness and the constant of uniaxial magnetic anisotropy by formulas, according to [34]:

$$A \approx \frac{3}{2}\frac{k_B T_N}{a_{Fe-Fe}}, \tag{4}$$

$$K_u = \frac{16AK^2(m)m}{\lambda^2}, \tag{5}$$

where k_B is the Boltzmann constant, a_{Fe-Fe} is interatomic distance, and T_N is the Néel temperature.

Table 2. Concentration dependences of the Néel temperature (the data were taken from [15]) of exchange hardness constant A, anharmonism parameter m, the first-order complete elliptic integral $K(m)$, magnetic uniaxial anisotropy constant K_u, and SSMS period λ [5] of multiferroics $BiFe_{1-x}Cr_xO_3$ (x = 0.05, 0.10, and 0.20)

x	T_N, K	A (10^{-6} erg/cm^3)	m	$K(m)$	λ (Å)	K_u (10^{-6} erg/cm^3)
0.00	643	3.33	0.10	1.61	620	0.36
0.05	608.5	3.15	0.26	1.69	620	0.99
0.10	580	3.00	0.49	1.85	620	2.08
0.20	510	2.64	0.78	2.22	620	4.22

Table 2 gives the values of the exchange hardness and the constant of uniaxial magnetic anisotropy. It was assumed that parameter $a_{Fe-Fe} = 4$ Å [35] and it is changed insignificantly in the perovskites under study. The concentration dependence of T_N in the $BiFe_{1-x}Cr_xO_3$ system in the range x = 0–0.20 is given in Table 2. These data were taken from [15]. The calculations were performed assuming that the cycloid length was $\lambda = 620 \pm 20$ Å, according to [5], and it was not dependent on the chromium content. We estimated the constant of uniaxial magnetic anisotropy K_u as a function of the chromium content in $BiFe_{1-x}Cr_xO_3$ (x = 0–0.20) by Eq. (5) using the parameter m and $K(m)$ from Table 2. At room temperature, $K_u \approx 0.36 \times 10^6$ erg/cm^3 at $x = 0$ and increased to $K_u \approx 4.22 \times 10^6$ erg/cm^3 at $x = 0.20$. Table 2 also gives the estimations of the constant of uniaxial magnetic anisotropy K_u and the exchange energy density E_{exch} as a function of the composition. As is seen from Table 2, the increase in anharmonism parameter m in the $BiFe_{1-x}Cr_xO_3$ system as the chromium concentration increased was mainly determined by the increase in the constant of uniaxial magnetic anisotropy K_u.

We suppose that the observed effects (the decrease in the crystal lattice parameters, HFMF on ^{57}Fe nuclei, and the constant of uniaxial magnetic anisotropy) were due to significant lattice distortions, because of the large difference of ionic radii and also the decrease in the number of d electrons in the electronic structure of the multiferroics $BiFe_{1-x}Cr_xO_3$ upon substituting of chromium atoms ($3d^3$) for iron atoms ($3d^5$) and, as a result, due to the change the bond angles and lengths in the Fe–O–Fe/Cr chains and also the change in the degree of the bond covalence.

4. CONCLUSIONS

The X-ray diffraction studies of the samples of the multiferroics $BiFe_{1-x}Cr_xO_3$ (x = 0.05, 0.10, and 0.20) prepared by solid-phase synthesis under high pressures showed that the crystal structure of the samples was rhombohedral with space group $R3c$. The lattice parameters decreased as the chromium concentration increased.

The Mössbauer spectroscopy at room temperature was used to study the influence of substitution of

Cr atoms for Fe atoms on the spatial spin-modulated structure and also the hyperfine electric and magnetic interactions of ^{57}Fe nuclei in the multiferroics $BiFe_{1-x}Cr_xO_3$ ($x = 0.05$, 0.10, and 0.20).

It was found that the structure of substituted ferrites contained the iron atom positions, the first coordination sphere of which contained from one to five chromium atoms in the dependence on the chromium content in the sample. Chromium atoms were randomly distributed over the iron atom positions.

The dependence of the isotropic contribution H_{is} to HFMF on the number N_{Cr} of Cr cations in the nearest environment of a Fe cation in the $BiFe_{1-x}Cr_xO_3$ ($x =$ 0.05, 0.10, and 0.20) was described in a linear approximation for the first three values of N_{Cr} (0, 1, 2). In this case, the substitution of Cr atom for Fe atom changed field H_{is} by $\Delta H_{is} \cong -21.6$ kOe. The anisotropic contributions H_{an} to HFMF were close and equal to $H_{an} = 4.5 \pm 0.2$ kOe. We did not observe noticeable changes in the anisotropic contribution, the quadrupole shift, and the Mössbauer line shift.

In the substituted ferrites, the anharmonic spin-modulated structure of cycloid type formed; in the structure, iron atoms with different cation environments took part. The anharmonism parameter linearly increased from $m = 0.10$ at $x = 0.00$ to $m = 0.78 \pm 0.02$ at $x = 0.20$. We estimated the constant of uniaxial magnetic anisotropy K_u as a function of the chromium content: at room temperature, $K_u \approx 0.36 \times 10^6$ erg/cm^3 at $x = 0$ and increased to $K_u \approx 4.22 \times 10^6$ erg/cm^3 at $x = 0.20$.

ACKNOWLEDGMENTS

This work was supported by the Russian Foundation for Basic Research (project no. 14-02-01109a) and the Ministry of Education and Science of the Russian Federation (project no. 3.5859.2017/8.9).

REFERENCES

1. G. A. Smolenskii and V. A. Bokov, J. Appl. Phys. **35**, 915 (1964).
2. H. Schmid, Ferroelectrics **162**, 317 (1994).
3. N. A. Hill, J. Phys. Chem. B **104**, 6694 (2000).
4. W. Eerenstein, N. D. Mathur, and J. F. Scott, Nature **442**, 759 (2006).
5. I. Sosnowska, T. Peterlin-Neumaier, and E. Steichele, J. Phys. C **15**, 4835 (1982).
6. C. Tabares-Munoz, J.-P. Rivera, A. Bezinges, A. Monnier, and H. Schmid, Jpn. J. Appl. Phys. **24**, 1051 (1985).
7. Yu. F. Popov, A. M. Kadomtseva, S. S. Krotov, D. V. Belov, G. P. Vorob'ev, P. N. Makhov, and A. K. Zvezdin, Low Temp. Phys. **27**, 478 (2001).
8. V. A. Khomchenko, M. Kopcewicz, A. M. L. Lopes, Y. G. Pogorelov, J. P. Araujo, J. M. Vieira, and A. L. Kholkin, J. Phys. D **41**, 102003 (2008).
9. V. A. Khomchenko, I. O. Troyanchuk, D. V. Karpinsky, and J. A. Paixão, J. Mater. Sci. **47**, 1578 (2012).
10. V. A. Khomchenko, L. C. J. Pereira, and J. A. Paixâo, J. Appl. Phys. **115**, 034102 (2014).
11. J. B. Goodenough, *Magnetism and the Chemical Bond* (Wiley, New York, 1963).
12. P. Baettig and N. Spaldin, Phys. Lett. **86**, 025505 (2005).
13. M. R. Suchomel, C. I. Thomas, M. Allix, M. J. Rosseinsky, A. M. Fogg, and M. F. Thomas, Appl. Phys. Lett. **90**, 112909 (2007).
14. F. G. Chang, N. Zhang, F. Yang, S. X. Wang, and G. L. Song, J. Phys. D **40**, 7799 (2007).
15. S. S. Arafat, Chin. Phys. B **23**, 066101 (2014).
16. Luo Bing-Cheng, Chen Chang-Le, Xu Zhi, and Xie Qian, Phys. Lett. A **374**, 4265 (2010).
17. J. B. Li, G. H. Rao, J. K. Liang, Y. H. Liu, J. Luo, and J. R. Chen, Appl. Phys. Lett. **90**, 162513 (2007).
18. S. Layek, S. Saha, and H. C. Verm, AIP Adv. **3**, 032140 (2013).
19. V. S. Rusakov, V. S. Pokatilov, A. S. Sigov, M. E. Matsnev, and T. V. Gubaidulina, JETP Lett. **100**, 463 (2014).
20. V. Rusakov, V. Pokatilov, A. Sigov, M. Matsnev, and T. Gubaidulina, J. Mater. Sci. Eng. B **4**, 302 (2014).
21. M. E. Matsnev and V. S. Rusakov, AIP Conf. Proc. **1489**, 178 (2012).
22. M. E. Matsnev and V. S. Rusakov, AIP Conf. Proc. **1622**, 40 (2014).
23. R. D. Shannon, Acta Crystallogr. A **32**, 751 (1976).
24. V. S. Rusakov, V. S. Pokatilov, A. S. Sigov, M. E. Matsnev, A. M. Gapochka, T. Yu. Kiseleva, A. E. Komarov, M. S. Shatokhin, and A. O. Makarova, Fiz. Tverd. Tela **58**, 102 (2016).
25. I. Sosnowska and A. K. Zvezdin, J. Magn. Magn. Mater. **140–144**, 167 (1995).
26. A. Palewicz, T. Szumiata, R. Przenioslo, I. Sosnowska, and I. Margiolaki, Solid State Commun. **140**, 359363 (2006).
27. R. R. Sharma, Phys. Rev. B **6**, 4310 (1972).
28. R. E. Watson and A. J. Freeman, Phys. Rev. **123**, 2027 (1961).
29. F. van der Woude, and G. A. Sawatzky, Phys. Rev. B **4**, 3159 (1971).
30. Nai Li Huang, R. Orbach, Šimakek, J. Owen, and D. R. Taylor, Phys. Rev. **156**, 383 (1967).
31. I. Sosnowska and A. K. Zvezdin, J. Magn. Magn. Mater. **140**, 167 (1995).
32. A. A. Belik, S. Iikubo, K. Kodama, N. Igawa, S. Shamoto, and E. Takayama-Muromachi, Chem. Mater. **20**, 3765 (2008).
33. C. Darie, C. Goujon, M. Bacia, H. Klein, P. Toulemonde, P. Bordet, and E. Syard, Solid State Sci. **12**, 660 (2010).
34. A. V. Zalesskii, A. K. Zvezdin, A. A. Frolov, and A. A. Bush, JETP Lett. **71**, 465 (2000).
35. J. M. Moreau, C. Michel, R. Gersdon, and W. J. James, J. Phys. Chem. Solids **32**, 1315 (1971).

Translated by Yu. Ryzhkov